Proceedings 10th NUMGE 2023
10th European Conference on Numerical Methods in Geotechnical Engineering
Zdravkovic L, Kontoe S, Taborda DMG, Tsiampousi A (eds)

© Authors: All rights reserved, 2023
https://doi.org/10.53243/NUMGE2023-47

Thermo-hydro-mechanical simulation of deep excavations in claystone

S. Tourchi[1], M. Mánica[2], A. Gens[3], J. Vaunat[3],

[1]*Institute of Hydrogeology, Engineering Geology and Applied Geophysics, Faculty of Science, Charles University, Prague, Czech Republic.*

[2]*Institute of Engineering, National Autonomous University of Mexico, Mexico City, Mexico.*

[3]*Department of Civil and Environmental Engineering, Universitat Politècnica de Catalunya, Barcelona Tech - CIMNE, Barcelona, Spain.*

ABSTRACT: The paper is centred on the enhancement of an existing hydro-mechanical model for argillaceous hard soils - weak rocks to provide predictive capability with respect to temperature evolution in the light of new experimental evidence. A number of developments of the original temperature-independent formulation are proposed. In particular, functions describing the yield locus, stiffness and strength parameters are improved to consider the elastic domain shrinking and the degradation of stiffness and strength parameters with temperature elevation. The developed thermo-mechanical constitutive model is applied, via a suitable coupled THM formulation, to the coupled THM analysis of an in-situ heating test performed in the Meuse/Haute-Marne Underground Research Laboratory. The relevance and importance of the temperature effect in the damaged zone around the in-situ heating tunnel are clearly demonstrated.

Keywords: Constitutive model; Thermal behaviour; Elastoplasticity; argillaceous materials.

1 INTRODUCTION

This contribution focused on the thermo-mechanical modelling of argillaceous hard soils - weak rocks, i.e., geological materials where fine-grained particles predominate (Gens, 2013). The tremendous interest in these materials lies in the fact that they are very desirable as potential host media for high-level radioactive waste (Tourchi, 2020). The temperature elevation might affect the crack network of the (excavation damage zone) EDZ and overall rock permeability in the close field, resulting in possible thermo-mechanical" failure. For a proper understanding and appropriate modelling of the excavation damaged zone around repository cells at elevated temperatures, the combined effects of thermo-hydro-mechanical (THM) phenomena should be considered in a constitutive model.

Several thermo-mechanical models that can reproduce most of the observed behaviour of saturated clays at elevated temperatures have been developed by several researchers. Hueckel and Borsetto (1990) developed one of the first models by extending the well-known Cam Clay model to consider thermo-elastoplastic behaviour. Their proposed model involves the shrinking of the elastic domain during heating (i.e., thermal softening) and its expansion during cooling when the stress path falls within the yield surface. In fact, adopting similar assumptions, most subsequent models are based on the same principle (Abuel-Naga et al., 2009; Cui et al., 2000; Di Donna and Laloui, 2015; Graham et al., 2001; Hamidi et al., 2017, 2015; Hamidi and Tourchi, 2018; Laloui and Francois, 2009; Modaressi and Laloui, 1997; Robinet et al., 1996; Tourchi and Hamidi, 2015; Yao and Zhou, 2013). In the meantime, the concept of bounding surface plasticity has also been extended to improve the modelling of cyclic behaviour at various temperatures and volume change under thermal loading at intermediately and highly overconsolidated states (Cheng et al., 2020; Di Donna and Laloui, 2015; Golchin et al., 2022, 2022; Laloui and Cekerevac, 2008; Laloui and François, 2009; Modaressi and Laloui, 1997; Zhou and Ng, 2018).

As noted in the previous paragraph, many of the thermo-mechanical are formulated in the framework of critical state concept and modified Cam-clay, in which thermo-plastic behaviour is incorporated using a temperature-dependent yield pressure. The latter is particularly suitable for normally consolidated (or lightly overconsolidated) soft clays, where their behaviour is controlled, to a large extent, by a volumetric yielding mechanism. However, this is not necessarily the case for indurated argillaceous materials, where strong post-sedimentation diagenetic bonds make the mobilisation of the shear resistance more likely in typical engineering applications, including deep tunnelling.

Mohr-Coulomb type of failure criterion, with two strength parameters to describe the plastic behaviour, is more appropriate for these endured rocks. When compared with the work on the thermo-mechanical modelling of clays, a limited number of thermo-mechanical models are developed for argillaceous rocks. The peculiarities of the mechanical response of argillaceous rocks to heating established in experiments consist of a thermal hardening, with an elastic thermal expansion observed below the maximum supported temperature, followed by a plastic contraction at yielding once the maximum temperature is reached, as well as more ductile behaviour with an apparent decrease in peak strength at elevated temperature.

Recent experimental findings led to the idea of extending a reference isothermal constitutive model (Mánica et al., 2017) to non-isothermal conditions. The core of the mechanical part of the reference model is taken from the Mohr-Coulomb yield criterion, which has been generalised to include anisotropy of strength and stiffness, behaviour nonlinearity and occurrence of plastic strains before peak strength, softening after the peak, time-dependent creep deformations and permeability increase due to damage in both saturated and unsaturated conditions. The proposed non-isothermal model consists of an elasticity law, plastic flow rule, hardening law, and yield condition. These elements are generalised to depend explicitly on temperature and suitably modified to reproduce the main features of the thermo-mechanical behaviour of the endured argillaceous rocks mentioned above. In the following sections, the proposed thermo-elastoplastic model is introduced. The proposed model is then applied to the THM modelling of an in-situ heating test carried out in Callovo-Oxfordian (COx) claystone in the Meuse/Haute-Marne underground research laboratory (Bumbieler et al., 2021; Tourchi et al., 2021, 2019a, 2019b).

2 THERMOPLASTICITY

There are quite comprehensive experimental data on the thermo-mechanical behaviour of clays. In general, heating a saturated clay under drained conditions induces strength and volumetric changes that depend on the clay's temperature and stress history condition. The temperature-induced volume change tends to be contractive and irreversible for normally consolidated clays, whereas it becomes reversible and expansive for highly overconsolidated clays. On the other hand, experimental data on the thermo-mechanical behaviour of argillaceous rocks are scarcer in the scientific literature.

The following main characteristics of the thermal behaviour of argillaceous rocks appear to be the most important (Liu et al., 2019; Mohajerani et al., 2014; Zhang et al., 2007): modification of mechanical behaviour; quantitatively, this corresponds to a continuous variation of mechanical characteristics (e.g., strength parameters and stiffness) with temperature, and qualitatively it represents a transition to more ductile behaviour, and temperature-induced reversible expansive strains followed, at some temperature value, by irreversible contracting strains.

2.1 Temperature-induced changes in strength parameters

With regard to thermal shear resistance changes in argillaceous rocks namely Opalinus clay and COx claystone, more ductile behaviour with an apparent decrease in strength at elevated temperature, initially observed by Zhang et al. (2007) on Opalinus clay was confirmed by Menaceur et al. (2015) on COx claystone. More recently, Liu et al. (2019) conducted a series of lateral decompression tests (LD) with constant mean stress ($p'_\circ = 12$ MPa) on the COx claystone samples. Reduction of the shear strength due to the increase in temperature was evidenced on COx claystone samples confirming previously obtained thermo-mechanical strength degradation performed in the conventional triaxial tests (Figure 1).

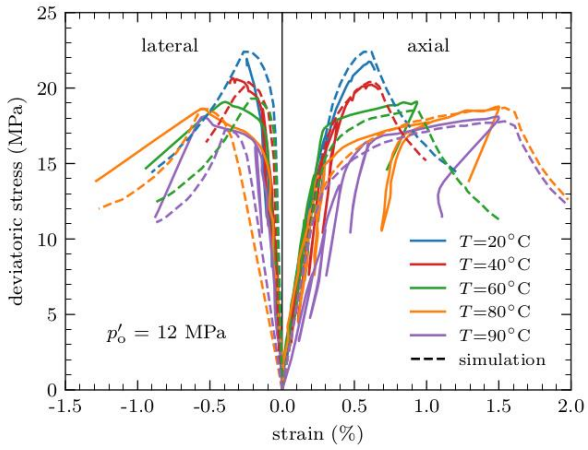

Figure 1. Results of lateral decompression tests at various temperatures on COx claystone samples.

Considering the thermal extension of the Mohr-Coulomb model, as a single yield surface plasticity, the material behaviour upon shearing depends on the strength parameters (internal friction angle and cohesion strength), which modify the yield locus. The thermal evolution of the internal friction angle is expressed using a linear relation as follows:

$$\varphi_{mob}(T) = \varphi(T_0)[1 - \alpha\, ln(T/T_0)] \qquad (1)$$

where $\varphi(T_0)$, $\varphi_{mob}(T)$ are the friction angle at the reference temperature (T_0) and elevated temperature (T). The coefficient α is a model parameter that controls the thermal evolution of the internal friction angle. The other parameter controlling the yield locus evolution is the cohesion strength which it is assumed that it varies

with temperature in the same way but not equal to the friction angle.

2.2 *Dependency law for the thermal evolution of stiffness*

All experiments noted above observed the reduction of Young's modulus with temperature increase. As shown in Figure 2 it appears that the *E-T* relationship for COx claystone can be normalised. The dashed lines are drawn using Equation (2) and interpolation of the laboratory data.

$$E(T) = E(T_0)[1 - \gamma\, ln(T/T_0)] \quad (2)$$

where $E(T_0)$ is Young's modulus at initial temperature (T_0.) and γ is a temperature-independent constant. The coefficient γ is the model constant that controls the thermal evolution of Young's modulus.

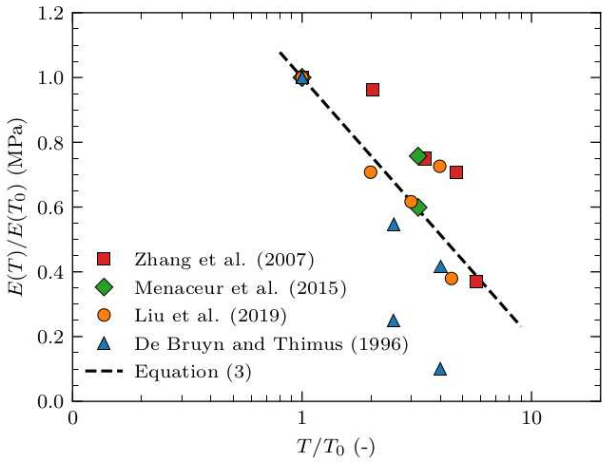

Figure 2. Normalised evolution of Young's modulus with temperature.

3 CONSTITUTIVE THERMO-ELASTOPLASTIC MECHANISM

The model presented here comprises two main deformation mechanisms: an instantaneous response related to stress and temperature change and a time-dependent response occurring under constant stress. The instantaneous response is described within the framework of elastoplasticity so that under low deviatoric stresses, the response is linear elastic but characterised through a transverse isotropic form of Hooke's law. For higher deviatoric stresses, plastic deformations can take place. An initial, a peak and a residual yield limit are considered. A generalised effective stress expression has been adopted here:

$$\boldsymbol{\sigma}' = \boldsymbol{\sigma} + S_e s B \mathbf{I} \quad (3)$$

where σ' is the effective stress tensor, σ is the total stress tensor, S_e is the equivalent degree of saturation (defined below), s is suction, B is Biot's coefficient, and $\mathbf{I}$ is the identity tensor. In the following, the term "stress" always denotes effective stress.

When there is unsaturation, the modified van Genuchten (van Genuchten, 1980) expression provides the retention curve that connects suction and equivalent degree of saturation, as shown below

$$S_e = \frac{S_l - S_{lr}}{S_{ls} - S_{lr}} = \left[1 + \left(\frac{S}{P}\right)^{\frac{1}{1-\lambda}}\right]^{-\lambda} \quad (4)$$

where S_l is the degree of saturation, S_{lr} is the residual degree of saturation, S_{ls} is the degree of saturation in saturated conditions (normally 1), and P and λ are model parameters.

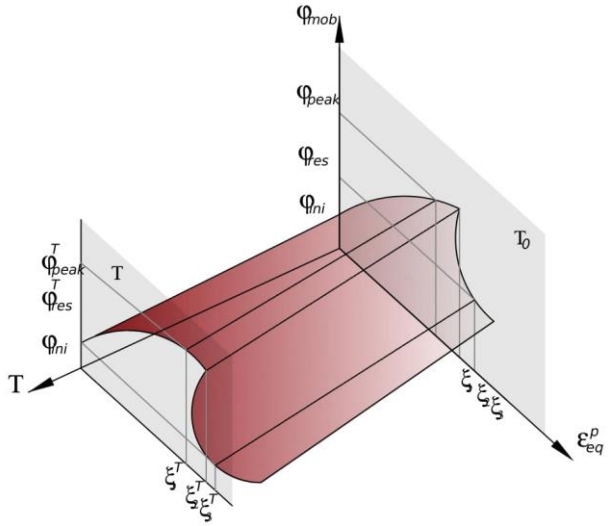

Figure 3. Mobilised friction angle as a function of temperature and plastic equivalent strain, ϵ_{eq}^{p}(Tourchi et al., 2022).

Cohesion evolves in parallel but not equal with the friction angle according to:

$$c_{mob}^{T} = c_{peak}^{T}\, cot\, \varphi_{ini}^{T_0}\, tan\, \varphi_{mob}^{T} \quad (5)$$

where c_{mob}^{T} is the mobilised cohesion at temperature T, c_{peak}^{T} is the peak cohesion, and $\varphi_{ini}^{T_0}$ and φ_{mob}^{T} are the initial and mobilised friction angles at initial and elevated temperatures, respectively. The Prager's consistency condition requires that, to maintain the yielding process,

$$df = \frac{\partial f}{\partial \boldsymbol{\sigma}'} : d\boldsymbol{\sigma}' + \frac{\partial f}{\partial \varphi} d\varphi + \frac{\partial f}{\partial c} dc = 0 \quad (6)$$

where

$$d\varphi = \frac{\partial \varphi}{\partial \varepsilon^p} \partial \varepsilon^p + \frac{\partial \varphi}{\partial T} dT \quad (7)$$

$$dc = \frac{\partial c}{\partial \varepsilon^p} \partial \varepsilon^p + \frac{\partial c}{\partial T} dT \quad (8)$$

Besides, a non-associated flow rule is adopted in the model. Rather than deriving a specific function for the

plastic potential, the flow rule is directly obtained from the yield criterion in the following way:

$$dg = \omega \frac{\partial f}{\partial p'}\frac{\partial p'}{\partial \boldsymbol{\sigma'}} + \frac{\partial f}{\partial J}\frac{\partial J}{\partial \boldsymbol{\sigma'}} + \frac{\partial f}{\partial \theta}\frac{\partial \theta}{\partial \boldsymbol{\sigma'}} = 0 \qquad (9)$$

where g, ω, θ *and* J are the plastic potential, a constant that controls the volumetric component of plastic deformations, Lode angle and deviatoric stress invariant. Hence, if the flow rule is assumed to be non-associated, that is if

$$d\boldsymbol{\varepsilon}^p = d\lambda \frac{\partial g}{\partial \boldsymbol{\sigma'}} \qquad (10)$$

As $d\varphi = d\varphi(d\,\varepsilon_{eq}^p, d\,T)$ and $dc = dc(d\,\varepsilon_{eq}^p, d\,T)$ the plastic multiplier λ, which controls the amount of the plastic strain rate, is affected by the change in φ and c (Tourchi et al., 2020):

$$d\lambda = \frac{1}{H}\left[\frac{\partial f}{\partial \boldsymbol{\sigma'}} : \boldsymbol{\sigma'} + \left(\frac{\partial f}{\partial \varphi}\frac{\partial \varphi}{\partial T} + \frac{\partial f}{\partial c}\frac{\partial c}{\partial T}\right) dT\right] \geq 0 \qquad (11)$$

$$H = -\frac{\partial f}{\partial \varphi}\frac{\partial g}{\partial \boldsymbol{\sigma'}}\frac{\partial \varphi}{\partial \varepsilon_v^p} + \frac{\partial f}{\partial c}\frac{\partial g}{\partial \sigma'}\frac{\partial c}{\partial \varepsilon_v^p} \qquad (12)$$

Therefore the plastic strain increment is affected by the thermal variation of internal friction and cohesion, as long as $\sigma' \neq 0$. Otherwise, this dependence disappears, as for both forms of the yield locus $\partial\varphi/\partial T = 0$ and $\partial c/\partial T = 0$.

$$\frac{d\varepsilon^p}{dT} = \frac{1}{H}\frac{\partial g}{\partial \sigma'}\left[\left(\frac{\partial f}{\partial \varphi}\frac{\partial \varphi}{\partial T} + \frac{\partial f}{\partial c}\frac{\partial c}{\partial T}\right)\right] \qquad (13)$$

3.1 Viscoplastic components

The time-dependent response is characterised by a modified form of Lemaitre's law.

$$d\varepsilon^{vp} = dt(\dot{\varepsilon}^{vp}) \qquad (14)$$

where $d\varepsilon^{vp}$ is the visco-plastic strain increment (time-dependent response), dt is the time increment and $\dot{\varepsilon}^{vp}$ is the visco-plastic strain rate tensor. It is assumed that visco-plastic deformations are mainly caused by deviatoric stresses, with strain rates given by:

$$\dot{\boldsymbol{\varepsilon}}^{vp} = \frac{2}{3}\frac{\dot{\varepsilon}^{vp}}{q}\boldsymbol{s} \qquad (15)$$

$$q = \left(\frac{3}{2}\boldsymbol{s} : \mathbf{s}\right)^{\frac{1}{2}} \qquad (16)$$

$$\dot{\varepsilon}^{vp} = \varpi\langle q - \sigma_s\rangle^n\left(1 - \varepsilon_{eq}^{vp}\right)^m \qquad (17)$$

where ϖ is a viscosity parameter, σ_s is a threshold from which viscoplastic strain is activated, $\langle\rangle$ are the Macaulay brackets, n and m are material constants and ε_{eq}^{vp} is the state variable of the time-dependent response given by:

$$\varepsilon_{eq}^{vp} = \int_0^t \left(\frac{2}{3}\dot{\boldsymbol{\varepsilon}}^{vp} : \dot{\boldsymbol{\varepsilon}}^{vp}\right)^{\frac{1}{2}} dt \qquad (18)$$

In this way, larger viscoplastic strain rates are obtained for higher deviatoric stresses, and those rates decrease as viscoplastic strains accumulate in time, as observed in laboratory tests (Souley et al., 2011).

4 IN-SITU HEATING TEST

In order to illustrate the applicability of the proposed model, a finite element simulation has been performed using the finite element software CODE_BRIGHT (Olivella et al., 1996). The coupled THM behaviour of the ALC1604 in situ heating test (Tourchi et al., 2021) has been simulated using a two-dimensional model domain. In this case, the model has been run for the section located at a distance into the tunnel of 17.5m which is the location of the three boreholes that contain six temperature sensors and piezometers. The model domain and the finite element mesh used are depicted in Figure 4. The model also incorporates the geometry of the sleeve and the air gap between the sleeve and the COx claystone.

An initial constant temperature of 21.8°C has been assumed throughout the geometry. An anisotropic lithostatic initial stress distribution has been prescribed. Values at the experiment level are 16.2 MPa, 12.4 MPa and 12.7 MPa for the vertical, major and minor horizontal components, respectively. A hydrostatic distribution of water pressure was initially defined, with a value equal to the field value (4.7 MPa) at the test level. Model parameters for the thermo-mechanical constitutive model can be found in Tourchi et al. (2021).

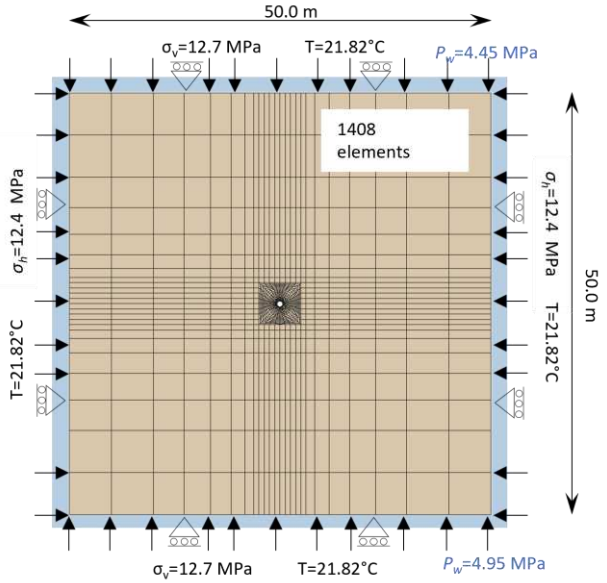

Figure 4. Domain, finite element mesh and boundary conditions.

4.1 Thermal results

The observed evolution of temperatures is shown in Figure 5 and compared with the results of the analyses using proposed non-isothermal model and reference model (Tourchi et al., 2021). It can be noted that, after about one year of heating, temperatures generally rise very slowly throughout the COx claystone. Moreover, anisotropic effects are noticeable, temperature along the bedding increases more rapidly than in the orthogonal direction.

4.2 Excavation damaged zone

The heat emitted by the high-level radioactive waste will increase the temperature in the host rock, with a maximum admitted temperature of 90°C around the waste canisters in the French concept. As stated above, the ALC1604 cell is parallel to the major horizontal stress (σ_H) and has a nearly isotropic stress state in the plane normal to the tunnel axis. Despite that, the EDZ extends further in the horizontal direction, suggesting strong anisotropic characteristics of the rock mass. The comparison of the computed plastic multiplier increments distributions at the end of heating with those obtained from the isothermal reference model is shown in Figure 6. Thermoplastic-induced fractures caused by EDZ extension during the heating phase are distinguished in the plots.

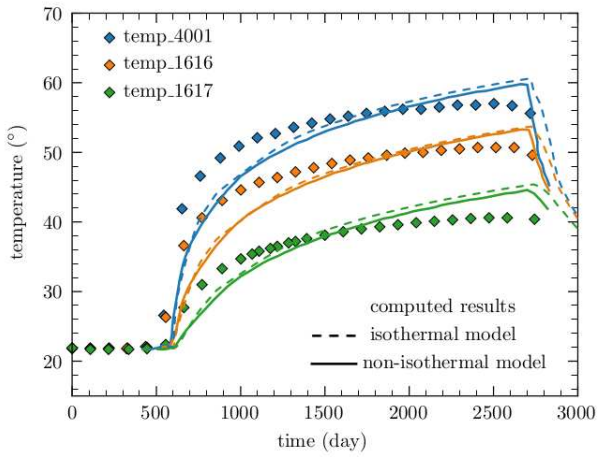

Figure 5. Evolution of temperatures in COx claystone, observations and computed results.

4.3 Pore pressures

The low permeability of COx claystone ensures that the resulting excess pore pressure does not dissipate rapidly. Figure 7 presents a comparison between the results of the analysis and pore pressure measurements. The results of the analysis using isothermal model have also been added. It is apparent that the pore pressure increase is reasonably well captured by the presented model for both excavation and heating phases. As shown in the figure, the closer to the plastic zone the point is, the more accurate the model result is, indicating that the proposed model is able to capture the main features of the mechanical and hydraulic behaviours associated with thermo-mechanical evolution of EDZ.

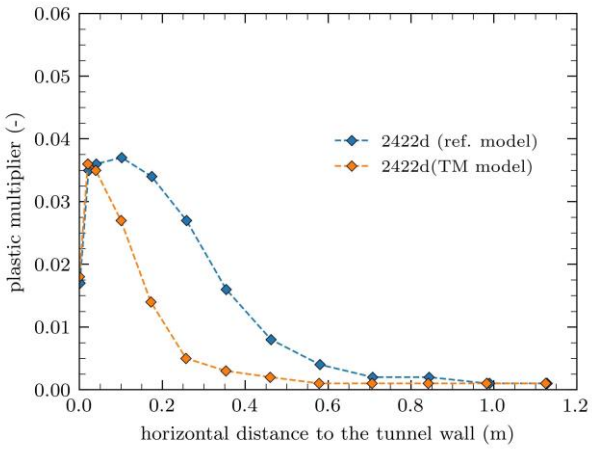

Figure 6. Computed plastic multiplier at the end of heating in the horizontal direction.

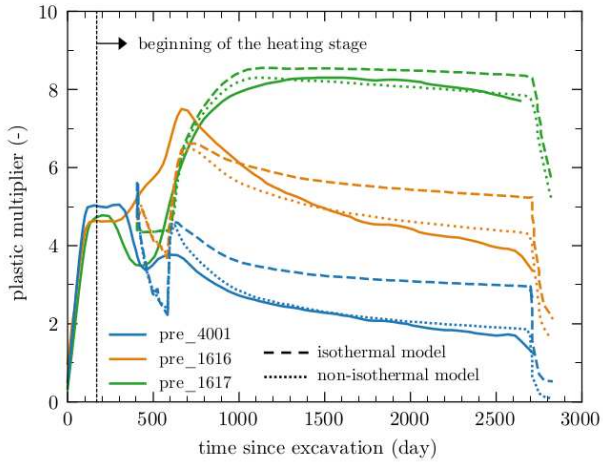

Figure 7. Evolution of pore pressure increments at various points in the COx claystone: observed and computed results.

5 CONCLUSIONS

This paper presents a thermo-mechanical model for argillaceous rocks developed within the framework of elastoplasticity that includes a number of features that are relevant for a satisfactory description of their thermo-mechanical behaviour. The comparison of the experimental data on COx claystone samples with the model predictions shows that all observed phenomena are correctly described. The constitutive model has then been applied to the analysis of the in-situ heating test conducted in the Meuse/Haute- Marne Underground Research Laboratory (MHM URL). The pattern of observed pore water pressure, as well as the damaged zone, are generally satisfactorily reproduced. It has been shown that it is essential to incorporate the thermal dependency of strength parameters and stiffness if the field observations, and pore pressures, are to be adequately represented.

6 ACKNOWLEDGEMENTS

Research leading to these results has received funding from the European Commission via a Marie Curie Fellowship awarded to Dr. Saeed Tourchi (Grant agreement ID: 101033084).

7 REFERENCES

Abuel-Naga, H.M., Pender, M., Bergado, D.T. Bouazza, A. 2009. Thermomechanical model for saturated clays. *Géotechnique* **59**, 273–278.

Bumbieler, F., Plúa, C., Tourchi, S. Vu, M.N., Vaunat, J., Gens, A., Armand, G. 2021. Feasibility of constructing a full-scale radioactive high-level waste disposal cell and characterization of its thermo-hydro-mechanical behavior. *Int. J. Rock Mech. Min. Sci*. **137**, 104555.

Cheng, W., Chen, R., Hong, P., Cui, Y., Pereira, J.-M. 2020. A two-surface thermomechanical plasticity model considering thermal cyclic behavior. *Acta Geotech*. **15**, 2741–2755.

Cui, Y.J., Sultan, N., Delage, P. 2000. A thermomechanical model for saturated clays. *Can. Geotech*. J. **37**, 607–620.

Di Donna, A., Laloui, L. 2015. Response of soil subjected to thermal cyclic loading: Experimental and constitutive study. *Eng. Geol*. **190**, 65–76.

Gens, A. 2013. On the hydromechanical behaviour of argillaceous hard soils-weak rocks. *Proceedings of the 15th European Conference on Soil Mechanics and Geotechnical Engineering*, 71-118.

Golchin, A., Vardon, P.J., Hicks, M.A. 2022. A thermo-mechanical constitutive model for fine-grained soils based on thermodynamics. *Int. J. Eng. Sci*. **174**, 103579.

Graham, J., Tanaka, N., Crilly, T., Alfaro, M. 2001. Modified Cam-Clay modelling of temperature effects in clays. *Can. Geotech. J*. **38**, 608–621.

Hamidi, A., Tourchi, S. 2018. A thermomechanical constitutive model for unsaturated clays. *Int. J. Geotech. Eng*. **12**, 185–199.

Hamidi, A., Tourchi, S., Kardooni, F. 2017. A critical state based thermo-elasto-plastic constitutive model for structured clays. *J. Rock Mech. Geotech. Eng*. **9**, 1094–1103.

Hamidi, A., Tourchi, S., Khazaei, C. 2015. Thermomechanical Constitutive Model for Saturated Clays Based on Critical State Theory. *Int. J. Geomech*. **15**, 04014038.

Laloui, L., Cekerevac, C. 2008. Non-isothermal plasticity model for cyclic behaviour of soils. *Int. J. Numer. Anal. Methods Geomech*. **32**, 437–460.

Laloui, L., Francois, B. 2009. ACMEG-T: Soil Thermoplasticity Model. *J. Eng. Mech*. **135**, 932–944.

Liu, Z., Shao, J., Xie, S., Conil, N., Talandier, J. 2019. Mechanical Behavior of Claystone in Lateral Decompression Test and Thermal Effect. *Rock Mech. Rock Eng*. **52**, 321–334.

Mánica, M., Gens, A., Vaunat, J., Ruiz, D.F. 2017. A time-dependent anisotropic model for argillaceous rocks. Application to an underground excavation in Callovo-Oxfordian claystone. *Comput. Geotech*. **85**, 341–350.

Menaceur, H., Delage, P., Tang, A.M., Conil, N. 2015. The thermo-mechanical behaviour of the Callovo-Oxfordian claystone. *Int. J. Rock Mech. Min. Sci*. **78**, 290–303.

Modaressi, H., Laloui, L. 1997. A thermo-viscoplastic constitutive model for clays. *Int. J. Numer. Anal. Methods Geomech*. **21**, 313–335.

Mohajerani, M., Delage, P., Sulem, J., Monfared, M., Tang, A.M., Gatmiri, B. 2014. The thermal volume changes of the callovo-oxfordian claystone. *Rock Mech. Rock Eng*. **47**, 131–142.

Olivella, S., Gens, A., Carrera, J., Alonso, E.E. 1996. Numerical formulation for a simulator (CODE_BRIGHT) for the coupled analysis of saline media. *Eng. Comput*. **13**, 87-112.

Robinet, J.C., Rahbaoui, A., Plas, F., Lebon, P. 1996. A constitutive thermomechanical model for saturated clays. *Eng. Geol*. **41**, 145–169.

Souley, M., Armand, G., Su, K., Ghoreychi, M. 2011. Modeling the viscoplastic and damage behavior in deep argillaceous rocks. *Phys. Chem. Earth Parts ABC, Clays in Natural & Engineered Barriers for Radioactive Waste Confinement.* **36**, 1949–1959.

Tourchi, S. 2020. THM analysis of argillaceous rocks with application to nuclear waste underground storage (Doctoral thesis). *TDX Tesis Dr. En Xarxa. Universitat Politècnica de Catalunya*.

Tourchi, S. Gens, A., Vaunat, J., Mánica, M. and Scaringi, G., 2020. A thermomechanical model for argillaceous rocks. *E3S Web of Conferences*, 205, 13014. EDP Sciences.

Tourchi, S., Hamidi, A. 2015. Thermo-mechanical constitutive modeling of unsaturated clays based on the critical state concepts. *J. Rock Mech. Geotech. Eng*. **7**, 193–198.

Tourchi, S., Malcom, M.A.M., Vaunat, J., Gens, A. 2022. A thermomechanical model for argillaceous hard soils - weak rocks: application to THM simulation of deep excavations in claystone. *EarthArXiv*.

Tourchi, S., Vaunat, J., Gens, A., Bumbieler, F., Vu, M.-N., Armand, G. 2021. A full-scale in situ heating test in Callovo-Oxfordian claystone: observations, analysis and interpretation. *Comput. Geotech*. **133**, 104045.

Tourchi, S., Vaunat, J., Gens, A., Vu, M.N., Bumbieler, F. 2019a. Thermo-Hydro-Mechanical Simulation of a Full-Scale Steel-Lined Micro-Tunnel Excavated in the Callovo-Oxfordian Claystone, *Complas 2019*, 544–552.

Tourchi, S., Vaunat, J., Gens, A., Vu, M.N., Bumbieler, F. 2019b. Coupled Thm Analysis of Long-Term Anisotropic Convergence in the Full-Scale Micro Tunnel Excavated in the Callovo-Oxfordian Argillite, *Coupled Problems 2019*, 292–299.

van Genuchten, M. 1980. A Closed-Form Equation for Predicting the Hydraulic Conductivity of Unsaturated Soils. S*oil Sci. Soc. Am. J*. **44**, 892–898.

Yao, Y. p., Zhou, A. n. 2013. Non-isothermal unified hardening model: a thermo-elasto-plastic model for clays. *Géotechnique* **63**, 1328–1345.

Zhang, C.L., Rothfuchs, T., Su, K., Hoteit, N. 2007. Experimental study of the thermo-hydro-mechanical behaviour of indurated clays. *Phys. Chem. Earth* **32**, 957–965.

Zhou, C., Ng, C.W.W. 2018. A new thermo-mechanical model for structured soil. *Géotechnique* **68**, 1109–1115.